ASME Journal of Heat Transfer

Special Issue

Micro/Nanoscale Heat Transfer International Conference

January 6-9, 2008, Tainan, Taiwan

HT-08-1152 (Research Paper)

Molecular Dynamics Based Analysis of Nucleation and Surface Energy of Droplets in Supersaturated Vapors of Methane and Ethane

Jadran Vrabec*, Martin Horsch, and Hans Hasse

Universität Stuttgart, Institute of Thermodynamics and Thermal Process Engineering, Pfaffenwaldring 9, 70569 Stuttgart, Germany

ABSTRACT

Homogeneous nucleation processes are characterized by the nucleation rate and the critical droplet size. Molecular dynamics (MD) simulation is applied for studying homogeneous nucleation during condensation of supersaturated vapors of methane and ethane. The results are compared to the classical nucleation theory (CNT) and the Laaksonen-Ford-Kulmala (LFK) model that introduces a size dependence of the specific surface energy. It is shown for the nucleation rate that the Yasuoka-Matsumoto method and the mean first passage time (MFPT) method lead to considerably differing results. Even more significant deviations are found between two other approaches to the critical droplet size, based on the maximum of the Gibbs free energy of droplet formation (Yasuoka-Matsumoto) and the supersaturation dependence of the nucleation rate (nucleation theorem). CNT is found to agree reasonably well with the simulation results, whereas LFK leads to large deviations at high temperatures.

* Corresponding author. Electronic address: vrabec@itt.uni-stuttgart.de

Keywords: phase transition, nucleation, molecular dynamics

INTRODUCTION

Nucleation processes in vapors at very high supersaturations, i.e. in the vicinity of the spinodal, cannot be studied with experimental methods, because they are very fast, exhibiting rates that exceed the range accessible to measurement. Homogeneous nucleation supposes the absence not only of microscopic particles, but also of confining walls, a condition that is hard to approximate in experiments.

However, understanding homogeneous nucleation is required to develop an accurate theoretical approach to nucleation that extends to more complex and technically more relevant heterogeneous systems [1, 2, 3]. MD simulations can well be used to investigate the condensation of homogeneous vapors at high supersaturations.

The nucleation rate J is influenced to a large extent by the surface energy of emerging droplets which also determines how many droplets are formed and from which size on they become stable. The accuracy of different theoretical expressions for the surface energy can be assessed by comparison to MD simulation results.

NUCLEATION THEORY

CNT was developed by Volmer and Weber [4] in the 1920s and further extended by many contributions during the following decades [5]. It is founded on the capillarity approximation: droplets emerging during nucleation are assumed to have the same thermodynamic properties as the saturated bulk liquid. In particular, the specific surface energy ε of the emerging nano-scaled droplets is assumed to be the surface tension γ_0 of the planar phase boundary in equilibrium. Laaksonen, Ford, and Kulmala [6] proposed a surface energy coefficient $\kappa(\imath)$ that depends on the number $\imath$ of molecules in the droplet, such that $\varepsilon = \kappa(\imath)\gamma_0$ with

$$\kappa(\imath) = 1 + \alpha_1(T)\imath^{-1/3} + \alpha_2(T)\imath^{-2/3}. \quad (1)$$

Tanaka *et al.* [7] found that this expression leads to nucleation rates which agree with their simulation results.

It was shown both theoretically [8, 9] and by simulation [10, 11] that the surface tension acting in the curved interface of nano-scaled droplets is actually lower than in a planar interface. Figure 1 shows plots of the surface energy coefficient $\kappa(\imath)$ for methane and ethane at different temperatures. At low temperatures, LFK does indeed yield lower

specific surface energies for $\imath \to 0$. However, at high temperatures of about 0.9 T_c, LFK assumes that small droplets have a *significantly higher* specific surface energy than the planar interface, cf. Fig. 1.

The Gibbs free energy of droplet formation

$$\Delta G = A\varepsilon - V\rho_d k_B T \ln S_\mu - G_1, \tag{2}$$

with respect to the Gibbs free energy G_1 of a single-molecule "droplet," is composed of the positive surface contribution as discussed above, where the surface area is given by A, and a negative contribution of the volume V, where ρ_d is the density of the droplet and S_μ is the supersaturation of the vapor in terms of the chemical potential [4, 5]. The relation between droplet size $\imath$, surface area A, and volume V is given by assuming that all droplets are exactly spherical and have the same density ρ_d as the saturated bulk liquid.

The number N of small droplets with a Gibbs free energy of formation ΔG in metastable equilibrium with a supersaturated vapor consisting of N_1 molecules is given by [4]

$$N = N_1 \exp\left(-\Delta G / k_B T\right). \tag{3}$$

For relatively large droplets, however, the steady state distribution that is established in the initial nucleation stage of a condensation process is dominated by non-equilibrium phenomena. The steady state probability $P(\imath)$ for a droplet to contain $\imath$ molecules can be related to the corresponding equilibrium probability $P_0(\imath)$ by

$$P(\imath) = \left(1 - J\int_1^\imath \frac{d\imath}{B(\imath)P_0(\imath)}\right) P_0(\imath), \tag{4}$$

as determined by Yasuoka and Matsumoto [12]. Therein, $B(\imath)$ is proportional to the frequency of size changes for a droplet containing $\imath$ molecules.

The critical droplet size $\imath^*$ is the number of molecules in a droplet for which the Gibbs free energy of formation assumes its maximal value ΔG^* [4, 13]. The height of this energy barrier is the most influential parameter on the nucleation rate [5]

$$J = N_1 \exp\left(-\Delta G^* / k_B T\right) A^* p^v \lambda h^{-1} Z\Theta, \tag{5}$$

according to CNT, where A^* is the surface area of a critical droplet, p^v is the pressure of the supersaturated vapor, λ is the thermal wavelength, Z is the Zel'dovich factor, and Θ is the non-isothermal factor.

SIMULATION METHOD

Both the critical droplet size [14, 15] and the nucleation rate [7, 12, 14, 16, 17, 18] can be determined by molecular simulation. After an initial period of equilibration, the steady state distribution of droplets is established. The equilibrium distribution can then be obtained by Eq. (4) which transforms to

$$P_0(\imath) = \exp\left(J \int_1^{\imath} \frac{d\imath}{B(\imath)P(\imath)} \right) P(\imath), \tag{6}$$

according to Yasuoka and Matsumoto [12]. This translates to values for ΔG, cf. Eq. (3), from which ΔG^* and $\imath^*$ can be determined [14]. An approximation for the critical droplet size is also given by the "nucleation theorem" [19]

$$\imath^* \approx \left(\frac{\partial \ln J}{\partial \ln S_\mu} \right)_T - 1. \tag{7}$$

Both of these methods for calculating $\imath^*$ require data on the nucleation rate J, i.e. the number of macroscopic droplets emerging per volume and time in a steady state at constant supersaturation. From an MD simulation of a supersaturated vapor, this rate can straightforwardly be extracted by counting the droplets that exceed a certain threshold size. This method was proposed by Yasuoka and Matsumoto [12] who found that as long as this threshold is significantly higher than the critical droplet size, its precise choice hardly affects the observed value of J.

Alternatively, the nucleation rate can also be estimated by fitting data on the mean first passage time, i.e. the temporal delay required for the first droplet of a given size to appear, to a predefined kinetic model [16].

To adequately evaluate these theories, it is furthermore necessary to determine the supersaturation in terms of the chemical potential

$$S_\mu = \exp\left(\frac{1}{k_B T} \int_{p_s}^{p^v} \frac{dp}{\rho} \right), \tag{8}$$

based on an integral between the saturated vapor pressure p_s and the supersaturated pressure p^v along the isotherm of the metastable vapor, where ρ is the density of the vapor. That integral can in principle be evaluated by extrapolating from the stable to the metastable regime. However, it is both more reliable and more consistent to interpolate between MD results for the density dependence of the supersaturated vapor pressure [20, 21]. An extended series of simulations including metastable states was recently carried out by Baidakov *et al.* [22] for the Lennard-Jones (LJ) fluid.

The present study of methane and ethane is based on MD simulation of supersaturated vapors. Methane was modeled as a simple LJ fluid with the size parameter σ_{LJ} = 3.7281 Å and the energy parameter ε_{LJ} / k_B = 148.55 K. For ethane, a rigid two-center LJ fluid model was used: both LJ centers had the parameters σ_{LJ} = 3.4896 Å and ε_{LJ} / k_B = 136.99 K with a distance of 2.3762 Å between them and a point quadrupole with a moment Q = 0.8277 DÅ in the center of mass. These models were presented in previous work [23] and shown to reproduce data on the vapor pressure with an error of 3% or less, while for other key properties of systems with vapor-liquid coexistence, such as the saturated liquid density and the enthalpy of vaporization, the deviations are even lower.

Since simulated inhomogeneous systems are particularly affected by the choice of the cutoff radius [24, 25], comparatively large values were specified in the present work: the cutoff radius was at least 1.75 nm for methane and 1.85 nm for ethane. All present MD simulations contained more than 100,000 molecules, which minimizes the influence of finite-size effects [16]. The simulations were conducted in the canonical ensemble, with constant number of molecules, volume, and temperature.

Based on these simulations, the critical droplet size was determined from ΔG maxima as well as the "nucleation theorem." The required nucleation rates, published separately [17], were obtained according to the Yasuoka-Matsumoto method [12] with sufficiently large threshold sizes. Additionally, a system below the triple point was simulated to compare a published nucleation rate based on the MFPT method [16] with the corresponding result of the Yasuoka-Matsumoto method.

SIMULATION RESULTS

Confirming the applicability of the Yasuoka-Matsumoto approach to the nucleation rate, Fig. 2 shows that larger droplets are formed at lower rates, but these rates are all within one order of magnitude [17]. This difference is negligible compared to the deviations observed for the theoretical predictions. Moreover, the pressure decreases over simulation time as more and larger droplets are formed and the vapor is depleted, which explains the lower rates observed at a later stage of the nucleation process.

Wedekind *et al.* [16] simulated supersaturated vapors of the LJ fluid – interpreted, in their case, as a model for argon – and determined nucleation rates according to the MFPT method. Converted to values for methane, the MFPT nucleation rate is 10^{31} $m^{-3}s^{-1}$ at 63.6 K and 0.1391 mol/l. In a present MD simulation with 1.26 million molecules at the same conditions, the rate of formation for droplets exceeding a size of ten molecules was found to be $6 \cdot 10^{30}$ $m^{-3}s^{-1}$. Data on larger droplets were insufficient to determine a nucleation rate. However, J must be even lower than that, because extremely small droplets are formed at higher rates than macroscopic ones [12]. Hence, the MFPT method overestimates the nucleation rate in this case by at least a factor two. This confirms results of Römer and Kraska [18] who observed a deviation of a factor of ten between the MFPT and Yasuoka-Matsumoto approach.

Plots of the Gibbs free energy of droplet formation for ethane at 280 K and different supersaturations are shown in Fig. 3. A maximum is clearly visible, if the equilibrium distribution is taken as a basis. For comparison, values estimated directly from the steady state, i.e. by assuming $P(\imath) = P_0(\imath)$ instead of Eq. (6), are indicated as well. These plots do not exhibit a maximum and, as expected, the steady state begins to diverge significantly from the equilibrium distribution only near the critical droplet size. The simulation results also show that both CNT and LFK are qualitatively correct in these cases. However, CNT underestimates ΔG while LFK overestimates it. Moreover, in both cases it is clearly visible that LFK is a good approximation for the smallest droplets that contain 20 or less molecules.

The nucleation rates from MD simulation confirm CNT, deviations are throughout lower than three orders of magnitude. The LFK model provides a better approach to systems at lower temperatures (Fig. 4), whereas near the critical point it leads to considerable deviations (Fig. 5).

Values of the critical droplet size obtained from ΔG maxima and the "nucleation theorem" are compared in Fig. 6. The results from both approaches deviate from each other roughly by a factor of two and the ΔG maxima agree particularly well with the LFK model.

CONCLUSION

The nucleation rate and the critical droplet size were studied for methane and ethane by MD simulation of supersaturated vapors. Different approaches for evaluating these simulations were compared with each other as well as with CNT and the LFK model.

Deviations in the order of a factor two were found both for the MFPT approach to the nucleation rate and for the estimate of the critical droplet size based on the "nucleation theorem" – with respect to the corresponding methods proposed by Yasuoka and Matsumoto [12]. It is safe to assume that both MFPT, which is based on a kinetic model with only three free parameters, and the "nucleation theorem," which neglects all influences on the nucleation rate except that of ΔG^*, are less accurate than their counterparts. A factor two is hardly relevant for practical purposes if it is applied to the nucleation rate, but in case of the critical droplet size such a deviation leads to qualitative errors. This is due to the fact that i^* is roughly proportional to ΔG^* which carries exponential weight in Eqs. (3) and (5) and similar expressions [4].

A particularly significant deviation was found between the nucleation rate from simulation and the LFK model at high temperatures. This may be due to the surface energy term of the LFK model which assumes an unphysical increase of the specific surface energy for small droplets at high temperatures; as Tolman [8] showed, the surface tension $(\partial G/\partial A)_{p,T}$ converges to zero for $A \to 0$. In particular, LFK overestimates ΔG^* at high temperatures and high supersaturations (conditions with $50 < i^* < 500$) which leads to the low predictions of J shown in Fig. 5.

However, for the Gibbs free energy of formation of extremely small droplets ($i < 25$), consisting of a few molecules only, the LFK model was found to be a good approximation even at high temperatures, although it assumes an unphysically high specific surface energy under these conditions.

This result can be explained by taking two phenomena into account: 1) All droplets are supposed to be exactly spherical, whereas the average area to volume ratio may actually be significantly increased for nano-scale droplets.

Considering this, one obtains a higher surface energy, even for lower surface tensions. 2) According to the capillarity approximation, the pressure inside a droplet is assumed to be the saturated vapor pressure p_s. On the other hand, the pressure is significantly increased due to the surface tension, which decreases the (negative) volume contribution to ΔG. This effect leads to a larger Gibbs free energy of droplet formation even if no additional surface effects are considered.

ACKNOWLEDGMENTS

The authors thank Martin Bernreuther (High Performance Computing Center Stuttgart), Rodrigo Escobar (Pontificia Universidad Católica de Chile), Amador Guzmán (Universidad de Santiago de Chile), Nicolas Schmidt and Jonathan Walter (Universität Stuttgart) as well as Andrea Wix (Universiät Karlsruhe) for valuable discussions, and Deutsche Forschungsgemeinschaft for funding SFB 716. The simulations were performed on the HP XC6000 super computer at the Steinbuch Centre for Computing, Karlsruhe under the grant MMSTP.

NOMENCLATURE

A	surface area
B	intensity of droplet size fluctuations
G	Gibbs free energy
G_1	Gibbs free energy of a single-molecule droplet
J	nucleation rate
N	number of droplets
N_1	number of vapor molecules
P	steady state probability
P_0	equilibrium probability
Q	quadrupole moment
S_μ	supersaturation (with respect to the chemical potential)
T	temperature
T_c	critical temperature
V	volume
Z	Zel'dovich factor
h	Planck constant
k_B	Boltzmann constant
p	pressure
p_s	saturated vapor pressure
p^v	supersaturated vapor pressure
Θ	non-isothermal factor
α_1 and α_2	parameters of the LFK model
γ	surface tension
γ_0	tension of the planar phase boundary

ε	specific surface energy (with respect to the surface area)
ε_{LJ}	energy parameter of the Lennard-Jones potential
ι	number of molecules in a droplet
κ	LFK surface energy coefficient
λ	thermal wavelength
ρ	density
ρ_d	density of a droplet
σ_{LJ}	size parameter of the Lennard-Jones potential
superscript *	properties of a critical droplet

REFERENCES

[1] Lee, S.-H., Reeves, J. M., Wilson, J. C., Hunton, D. E., Viggiano, A. A., Miller, T. M., Ballenthin, J. O., and Lait, L. R., 2003, "Particle Formation by Ion Nucleation in the Upper Troposphere and Lower Stratosphere," Science, **301**, pp. 1886-1889.

[2] Määtänen, A., Vehkamäki, H., Lauri, A., Merikallio, S., Kauhanen, J., Savijärvi, H., and Kulmala, M., 2005, "Nucleation Studies in the Martian Atmosphere," J. Geophys. Res., **10**, E02002.

[3] Curtius, J., 2006, "Nucleation of Atmospheric Aerosol Particles," Comptes Rendus Phys., **7**, pp. 1027-1045.

[4] Volmer, M., and Weber, A., 1926, "Keimbildung in übersättigten Gebilden," Z. Phys. Chem. (Leipzig), **119**, pp. 277-301.

[5] Feder, J., Russell, K. C., Lothe, J., and Pound, G. M., 1966, "Homogeneous Nucleation and Growth of Droplets in Vapours," Adv. Phys., **15**(1), pp. 111-178.

[6] Laaksonen, A., Ford, I. J., and Kulmala, M., 1994, "Revised Parametrization of the Dillmann-Meier Theory of Homogeneous Nucleation," Phys. Rev. E, **49**(6), pp. 5517-5524.

[7] Tanaka, K. K., Kawamura, K., Tanaka, H., and Nakazawa, K., 2005, "Tests of the Homogeneous Nucleation Theory with Molecular-Dynamics Simulations," J. Chem. Phys., **122**, 184514.

[8] Tolman, R. C., 1949, "The Effect of Droplet Size on Surface Tension," J. Chem. Phys., **17**(3), pp. 333-337.

[9] Kirkwood, J. G., and Buff, F. P., 1949, "The Statistical Mechanical Theory of Surface Tension," J. Chem. Phys., **17**(3), pp. 338-343.

[10] Vrabec, J., Kedia, G. K., Fuchs, G., and Hasse, H., 2006, "Comprehensive Study on Vapour-Liquid Coexistence of the Truncated and Shifted Lennard-Jones Fluid Including Planar and Spherical Interface Properties," Mol. Phys., **104**(9), pp. 1509-1527.

[11] Napari, I., and Laaksonen, A., 2007, "Surface Tension and Scaling of Critical Nuclei in Diatomic and Triatomic Fluids," J. Chem. Phys., **126**, 134503.

[12] Yasuoka, K., and Matsumoto, M., 1998, "Molecular Dynamics of Homogeneous Nucleation in the Vapor Phase," J. Chem. Phys., **109**(19), pp. 8451-8470.

[13] Haber, F., 1922, "Über amorphe Niederschläge und krystallisierte Sole," Berichte der Deutschen Chemischen Gesellschaft B, **55**, pp. 1717-1733.

[14] Matsubara, H., Koishi, T., Ebiskuzaki, T., and Yasuoka, K., 2007, "Extended Study of Molecular Dynamics Simulation of Homogeneous Vapor-Liquid Nucleation of Water," J. Chem. Phys., **127**, 214507.

[15] Nellas, R. B., Chen, B., and Siepmann, J. I., 2007, "Dumbbells and Onions in Ternary Nucleation," Phys. Chem. Chem. Phys., **9**, pp. 2779-2781.

[16] Wedekind, J., Reguera, D., and Strey, R., 2006, "Finite-size Effects in Simulation of Nucleation," J. Chem. Phys., **125**, 214505.

[17] Horsch, M., Vrabec, J., Bernreuther, M., Grottel, S., Reina, G., Wix, A., Schaber, K., and Hasse, H., 2008, "Homogeneous Nucleation in Supersaturated Vapors of Methane, Ethane, and Carbon Dioxide Predicted by Brute Force Molecular Dynamics," J. Chem. Phys., **128**, 164510.

[18] Römer, F., and Kraska, T., 2007, "Homogeneous Nucleation and Growth in Supersaturated Zinc Vapor Investigated by Molecular Dynamics Simulation," J. Chem. Phys., **127**, 235409.

[19] Oxtoby, D. W., and Kashchiev, D., 1994, "A General Relation Between the Nucleation Work and the Size of the Nucleus in Multicomponent Nucleation," J. Chem. Phys., **100**(10), pp. 7665-7671.

[20] Linhart, A., Chen, C., Vrabec, J., and Hasse, H., 2005, "Thermal Properties of the Metastable Supersaturated Vapor of the Lennard-Jones Fluid," J. Chem. Phys., **122**, 144506.

[21] Nie, C., Geng, J., and Marlow, W. H., 2008, “Study of Thermal Properties of the Metastable Supersaturated Vapor with the Restricted Ensemble,” Physica A, **387**, pp. 1433-1438.

[22] Baidakov, V. G., Protsenko, S. P., and Kozlova, Z. R., 2008, “Thermal and Caloric Equations of State for Stable and Metastable Lennard-Jones Fluids: I. Molecular-dynamics Simulations,” Fluid Phase Equilib., **263**, pp. 55-63.

[23] Vrabec, J., Stoll, J., and Hasse, H., 2001, “A Set of Molecular Models for Symmetric Quadrupolar Fluids,” J. Phys. Chem. B., **105**(48), pp. 12126-12133.

[24] Trokhymchuk, A., and Alejandre, J., 1999, “Computer Simulations of Liquid/Vapor Interface in Lennard-Jones Fluids: Some Questions and Answers,” J. Chem. Phys., **111**(18), pp. 8510-8523.

[25] Shen, V. K., Mountain, R. D., and Errington, J. R., 2007, “Comparative Study of the Effect of Tail Corrections of Surface Tension Determined by Molecular Simulation,” J. Phys. Chem. B, **111**(22), pp. 6198-6207.

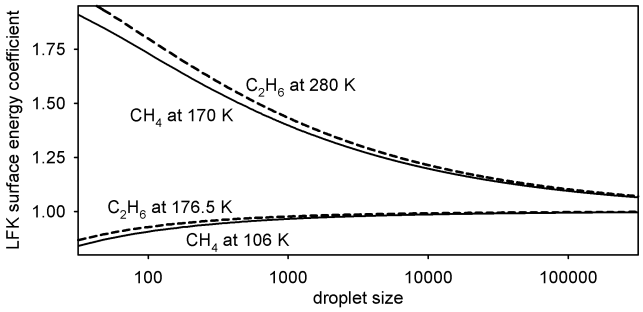

Fig. 1 Dependence of the LFK surface energy coefficient $\kappa(\iota)$ for methane (—) and ethane (- - -) on the droplet size ι

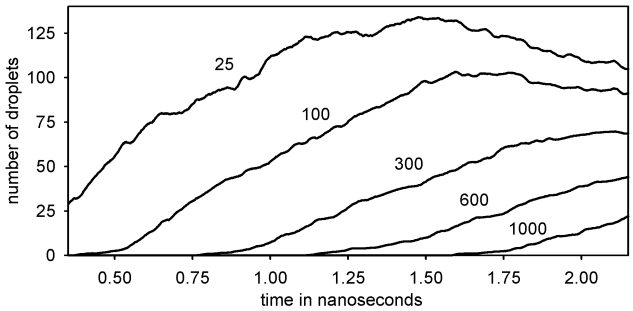

Fig. 2 Number of droplets containing at least 25, 100, …, 1000 molecules over simulation time [17]. Methane was regarded at 130 K and 1.606 mol/l in a volume of $(63.7\ \text{nm})^3$

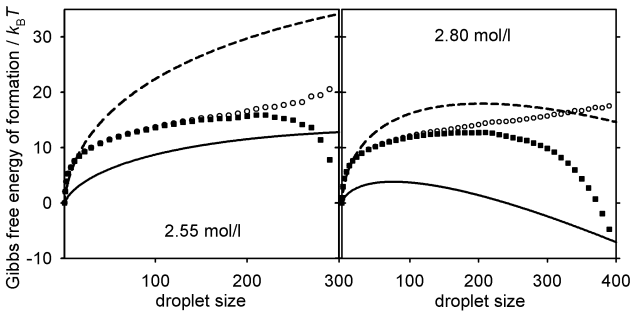

Fig. 3 **Dependence of the Gibbs free energy of droplet formation on the droplet size for ethane at 280 K and two different densities, calculated from the metastable equilibrium (■) and the steady state distribution (o) as well as CNT (—) and LFK (- - -)**

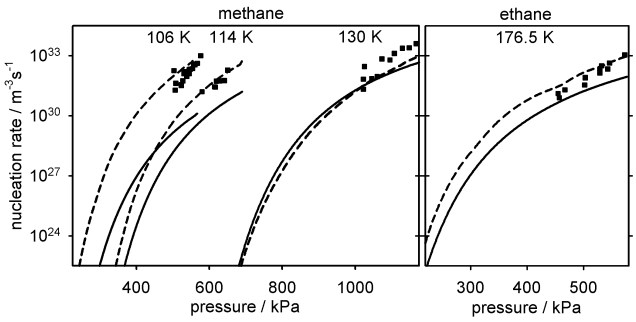

Fig. 4 **Nucleation rates of methane and ethane at low temperatures from simulation [17] determined according to the Yasuoka-Matsumoto method with different threshold sizes (■) as well as CNT (—) and LFK (- - -)**

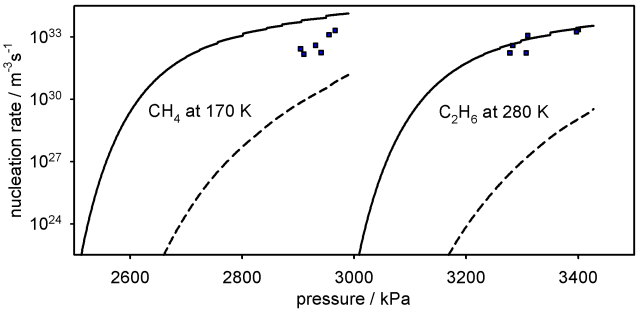

Fig. 5 **Nucleation rates of methane and ethane at high temperatures (0.89 and 0.92 T_c) from simulation [17] according to the Yasuoka-Matsumoto method with different threshold sizes (■) as well as CNT (—) and LFK (- - -)**

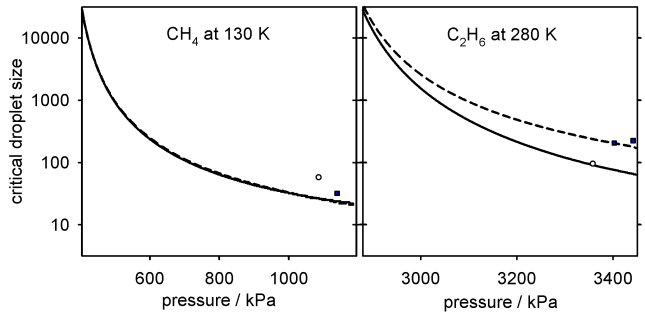

Fig. 6 **Critical droplet size for methane and ethane from maxima of the Gibbs free energy of droplet formation (■) and the supersaturation dependence of the nucleation rate (o) as well as CNT (—) and LFK (- - -)**

LIST OF FIGURE CAPTIONS

Fig. 1 Dependence of the LFK surface energy coefficient $\kappa(\iota)$ for methane (—) and ethane (- - -) on the droplet size ι

Fig. 2 Number of droplets containing at least 25, 100, …, 1000 molecules over simulation time [17]. Methane was regarded at 130 K and 1.606 mol/l in a volume of $(63.7\ \mathrm{nm})^3$

Fig. 3 Dependence of the Gibbs free energy of droplet formation on the droplet size for ethane at 280 K and two different densities, calculated from the metastable equilibrium (■) and the steady state distribution (o) as well as CNT (—) and LFK (- - -)

Fig. 4 Nucleation rates of methane and ethane at low temperatures from simulation [17] determined according to the Yasuoka-Matsumoto method with different threshold sizes (■) as well as CNT (—) and LFK (- - -)

Fig. 5 Nucleation rates of methane and ethane at high temperatures (0.89 and 0.92 T_c) from simulation [17] according to the Yasuoka-Matsumoto method with different threshold sizes (■) as well as CNT (—) and LFK (- - -)

Fig. 6 Critical droplet size for methane and ethane from maxima of the Gibbs free energy of droplet formation (■) and the supersaturation dependence of the nucleation rate (o) as well as CNT (—) and LFK (- - -)

LIST OF TABLE CAPTIONS

The submission does not contain any tables.